Journal of Chromatography, 647 (1993) 79–90
Elsevier Science Publishers B.V., Amsterdam

CHROMSYMP. 2786

Particle beam liquid chromatography–mass spectrometry behaviour of polynuclear metal carbonyl compounds

M. Careri*, A. Mangia, P. Manini and G. Predieri

Istituto di Chimica Generale ed Inorganica, Università di Parma, Viale delle Scienze, 43100 Parma (Italy)

V. Raverdino and G. Tsoupras

Hewlett-Packard S.A., Rue de Veyrot 39, 1217 Meyrin 1 (Switzerland)

E. Sappa

Dipartimento di Chimica Inorganica, Chimica Fisica e Chimica dei Materiali, Università di Torino, Via P. Giuria 7, 10125 Turin (Italy)

ABSTRACT

High-performance liquid chromatography (HPLC)–mass spectrometry (MS) was applied to organotransition-metal chemistry with the aim of studying the relationship between chromatographic behaviour and structural features of polynuclear organometallic compounds and of developing the methodological aspects of application of the combined technique in this field. In order to obtain significant structural information about organometallic compounds separated by HPLC, a particle beam LC–MS interface was used. As a first approach, some alkyne-carbonyl ruthenium derivatives and cyclopentadienyl nickel–ruthenium and nickel–osmium carbonyl clusters were considered; all these compounds are of relevant interest in the field of both homogeneous and heterogeneous catalysis. The separation of all the examined clusters was performed under reversed-phase conditions with non-aqueous mobile phases. Full-scan electron impact and chemical ionization mass spectra were obtained from the LC eluates.

INTRODUCTION

The on-line coupling of HPLC–MS was used in a research programme with the aim of studying the relationship between structure and chromatographic behaviour of polynuclear organometallic compounds and, more generally, to develop the methodological aspects of the application of this technique in organometallic chemistry, a field of great interest from the industrial, environmental and toxicological points of view.

Chromatographic techniques are widely used to separate and purify complex mixtures of organometallic compounds in preparative procedures; for this purpose column and thin-layer chromatography are used in most cases. From the analytical point of view, it has been proved that HPLC has great capability even in this field: in fact, HPLC allows rapid and adequately efficient separations of a large number of organometallic compounds, including homo- and heterometallic clusters of different nuclearity [1–5].

HPLC makes use of a variety of sensitive, liquid-phase detectors such as the spectrophotometric, fluorimetric and amperometric

* Corresponding author.

0021-9673/93/$06.00

ones. Owing to the structural complexity of the above substances, these detectors give scant information about the nature of the compounds in the column eluates. Moreover, since conventional HPLC does not provide the high efficiency available from capillary GC, LC chromatograms may contain unresolved peaks that non-specific detectors cannot differentiate. In this context the need for a more sensitive and specific detection system has generated considerable interest in developing the on-line LC–MS technique: mass spectrometry is an excellent tool for analyte identification and structural confirmation in chemical analysis. LC–MS allows the separation and identification of non-volatile, polar compounds, providing structural information for mixtures of components not suitable for GC–MS.

Although LC–MS has been applied extensively in the organic and biochemical analysis [6–11], the field of organotransition-metal chemistry is as yet unexplored with regard to this coupled technique. The problems associated with the interfacing of these two techniques are considerable, but recently there has been significant progress towards their solution. Furthermore, there is a need for structurally useful fragmentations (such as electron impact-like fragmentation) from LC–MS experiments: thermospray LC–MS and LC–atmospheric pressure ion source MS provide very mild ionization, resulting in a limited fragmentation and in a poor mass spectral specificity; nevertheless, thermospray provides more analytical information than other conventional LC detectors and it proves helpful for the characterization of unknown compounds also having high molecular mass, together with other analytical information that may be available.

The possibility of obtaining electron impact (EI) mass spectra, rich in structurally significant fragmentations, is provided by the recent MAGIC (monodisperse aerosol generation for introduction of liquid chromatographic effluents) and particle beam (PB) interfaces; chemical ionization (CI) mass spectra are also available from these interface devices.

With the aim of achieving significant structural information about organometallic compounds separated by HPLC, a particle beam LC–MS interface was used. Full-scan EI and CI mass spectra were obtained from three groups of carbonyl clusters: two groups made up of hydrido-acetylido carbonyl triruthenium clusters, deriving from the basic triangular metal framework $HRu_3(C{\equiv}CR)(CO)_9$. The first one was obtained from the cluster $HRu_3(C{\equiv}C\text{-}tert.\text{-}Bu)(CO)_9$ through substitution of the carbonyl ligands by group 15 donor ligands EPh_3 (E = P, As, Sb). The second one was obtained by varying the R acetylenic substituent in the parent cluster [R = iso-Pr, *tert.*-Bu, $C(Me)_2OH$,

TABLE I

FORMULAS, STRUCTURES AND MOLECULAR MASSES OF THE CLUSTERS

Compound		Mol. mass
	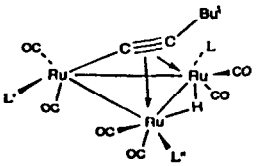	
I	L = L′ = L″ = CO	637.45
IIa	L = L″ = CO, L′ = PPh_3	871.73
IIb	L = L″ = CO, L′ = $AsPh_3$	915.68
IIc	L = L″ = CO, L′ = $SbPh_3$	962.50
III	L = CO, L′ = L″ = PPh_3	1106.01
IV	L = L′ = L″ = PPh_3	1340.29
	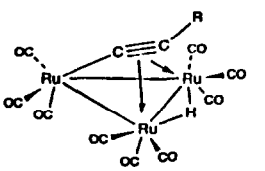	
V	R = iso-Pr	623.42
VI	R = $C(Me)_2OH$	639.42
VII	R = C(Me)(Ph)OH	701.49
	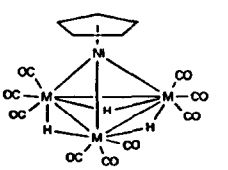	
VIII	M = Os	682.11
IX	M = Ru	949.50

C(Me)(Ph)OH]. In the third group, the tetrahedral cyclopentadienyl-hydrido nickel–osmium and nickel–ruthenium carbonyl clusters (η-C_5H_5)$NiM_3(\mu_2$-H)$_3(CO)_9$ [M = Os, Ru] were also considered.

All these compounds are of relevant interest in the field of both homogeneous and heterogeneous catalysis. The schemes of the structures of these complexes are reported in Table I, together with the respective formulas and the molecular masses.

Mass spectra of some acetylenic derivatives of iron and ruthenium carbonyl have been reported [12–15]; the spectra have been obtained for the single compounds, using a direct insertion probe.

The chromatographic behaviour of mono- and polynuclear metal clusters has been already intensively investigated [2–4,16] with the aim of studying the influence of the steric and electronic features on the retention and of verifying the analytical applications of HPLC in this field.

In this paper the results of the use of the on-line HPLC–MS in the separation and identification of the polynuclear carbonyl compounds are reported; these results demonstrate the application capabilities of this combined technique even in the field of organometallic chemistry.

EXPERIMENTAL

Compound $HRu_3(C{\equiv}C$-*tert.*-Bu)$(CO)_9$ (I) and its monosubstitution products with the EPh_3 ligand (IIa–IIc) were prepared as described in the literature for the derivative having E = P [17]. The triphenylphosphine di- and trisubstituted clusters were obtained, purified and identified as reported earlier [16]. Other acetylido derivatives (V–VII) were obtained from the corresponding alkynes using the same synthetic procedure described for I. Nickel–osmium and nickel–ruthenium clusters were synthesized by applying established methods [15,18].

HPLC conditions

The HPLC system consisted of a Hewlett-Packard Model HP1090 chromatograph (Palo Alto, CA, USA), equipped with a Rheodyne 7125 injector. A stainless-steel column (25 cm × 0.4 cm I.D.) filled with 5-μm LiChrosorb RP-18 (Merck, Darmstadt, Germany) was used. In order to check the maintenance of chromatographic resolution, a Perkin Elmer (Norwalk, CT, USA) LC-75 variable-wavelength UV–Vis detector was used, monitoring the eluates at 254 or 265 nm, depending on the position of the absorption maxima; acetonitrile solutions of the compounds (20 μl) were injected. The amounts of metal injected ranged between 0.1 and 0.5 μg when UV detection was used and between 0.5 and 5 μg in LC–MS mode. The flow-rate was 0.8 cm^3/min and 1 cm^3/min in the case of separations obtained in LC–MS and LC-UV mode, respectively. An acetonitrile–methanol (80:20) mixture was used for the isocratic elution of the first and the second set of clusters. Methanol was utilized as eluent for the separation of heterometallic complexes VIII and IX. In every case, data based on injections in flow injection analysis mode were primarily achieved, using methanol as mobile phase at 0.4 cm^3/min.

The solvents used were HPLC grade (Carlo Erba, Milan, Italy).

Interface conditions

A Hewlett-Packard Model HP 59980A particle beam LC–MS interface was used. The nebulizing gas was high-purity helium maintained at 50 p.s.i. (1 p.s.i. = 6894.76 Pa); the desolvation chamber temperature was held at 55°C. The particle beam nebulizing conditions were chosen first by injection of a test solution of benzidine (20 ng/μl in acetonitrile) supplied by Hewlett-Packard and then optimized with the studied compounds.

MS conditions

The mass spectrometer was a Hewlett-Packard Model HP5989A; the HP MS engine was equipped with a dual EI–CI ion source, a hyperbolic quadrupole mass analyser, a continuous dynode electron multiplier detector and a differentially pumped vacuum system with diffusion pumps. The HP MS 59940A ChemStation (HP-UX series) was used as analytical workstation.

Both EI and CI sources were utilized. The optimum source temperature was chosen within the range 250–320°C as a compromise between lower values for abundant molecular ions in the

spectrum and higher temperatures for total ion abundance. The overall best source temperature was 260°C. Using the electron impact source, mass spectra were obtained under these conditions: ionization energy of 30 eV and electron multiplier of 2300 V. In CI data acquisition, methane–ammonia (95:5) mixture was used as the reagent gas; in this case the ionization energy was 230 eV and the voltage applied to the electron multiplier was 2100 V. Both positive and negative ions were monitored in the CI mode.

The quadrupole temperature was held at 100°C.

For scan acquisition the system was scanned from 150 to 750 μ for compounds I and V–VII, from 250 to 1350 μ for compounds I–IV and from 100 to 980 μ for the heterometallic clusters VIII and IX.

RESULTS AND DISCUSSION

For preliminary adjustment of operating conditions flow injection analysis (FIA) was used, by injecting solutions of individual compounds into a mobile phase from an HPLC pump and transferring the mixture into the LC–PB-MS system, without the HPLC column. However, since overall system performance is controlled by the chromatographic conditions (type of column, variable eluent compositions for gradient elution), final optimization was carried out using the LC column.

With regard to the interface tuning, a determining factor of adjustment was found to be

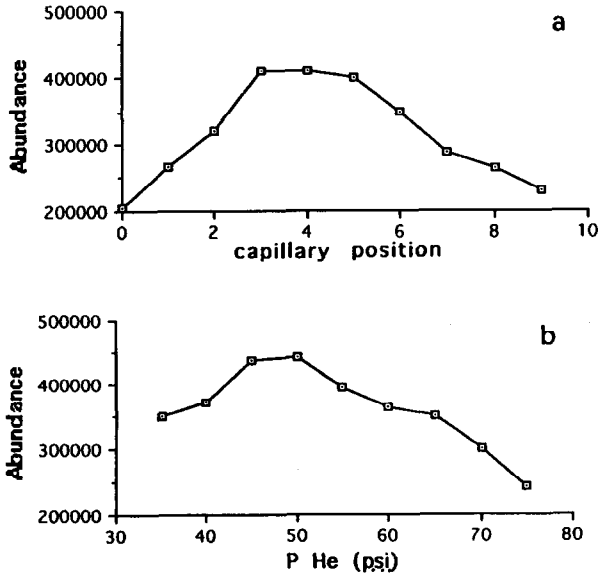

Fig. 1. Effect on peak abundance of $HRu_3(C{\equiv}C\text{-}tert.\text{-}Bu)(CO)_9$ of: (a) position of the end of the capillary in the nebulizer (arbitrary setting units); (b) nebulizing gas helium pressure. Operating conditions: FIA; eluent, methanol; flow-rate, 0.4 cm^3/min; source temperature, 260°C.

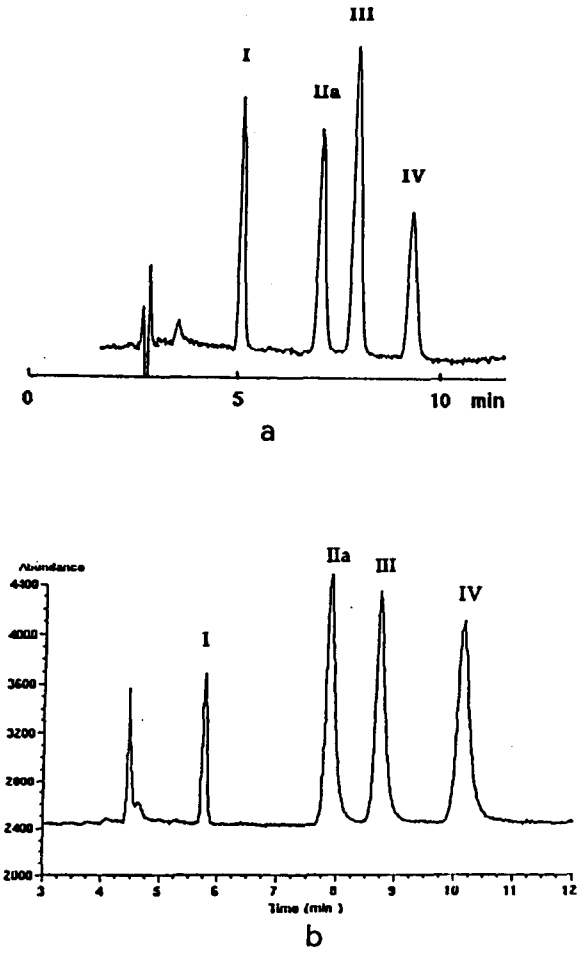

Fig. 2. Comparison of chromatograms of the cluster mixture I–IV with: (a) UV detection, $\lambda = 265$ nm; (b) MS detection, TIC signal. Chromatographic conditions: column, LiChrosorb RP-18; mobile phase, acetonitrile–methanol (80:20); flow-rate, 1.0 cm^3/min for LC–UV, 0.8 cm^3/min for LC–MS. MS conditions: CI source; source temperature, 260°C; reagent gas, methane–ammonia (95:5); scan range, 250–1350 μ; ionization energy, 230 eV, negative-ion signal.

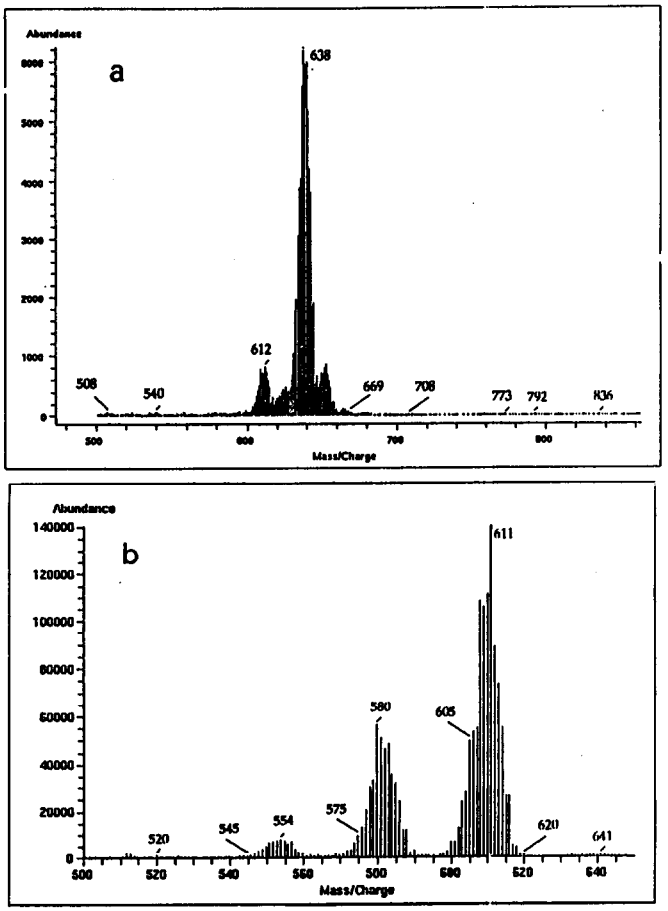

Fig. 3. LC–CI-MS spectra of $HRu_3(C{\equiv}C\text{-}tert.\text{-}Bu)(CO)_9$: (a) positive-ion signal; (b) negative-ion signal. Conditions as in Fig. 2.

the position of the end of the fused-silica capillary in the nebulizer, resulting in a different signal intensity for all compounds. The helium flow-rate in creating the aerosol in the interface was also found to affect sensitivity significantly, the optimum flow-rate being about 2 l/min. The effect of the variations in capillary position and of the helium flow-rate on the signal intensity is represented in Fig. 1 for the compound $HRu_3(C{\equiv}C\text{-}tert.\text{-}Bu)(CO)_9$, which was chosen as the reference compound. Of minor importance was the desolvation chamber temperature in the normal operating range 50–70°C, which was held constant at 55°C.

All the examined clusters were separated under reversed-phase conditions with non-aqueous mobile phases. The most efficient separations were obtained using a standard column (25 cm × 0.4 cm) requiring LC flows higher than those normally accommodated (0.4–0.5 cm^3/min) for the PB interface nebulizer. However, even though the optimum signal intensity was found to be in correspondence with 0.3–0.4 cm^3/min flow-rates, only a slight reduction in sensitivity was observed at a flow-rate of 0.8 cm^3/min. With regard to the solvent composition, methanol or acetonitrile–methanol mixtures were utilized for the elution of the organometallic compounds. In agreement with the results reported by other authors [19], under FIA conditions and at a flow-rate of 0.4 cm^3/min, a slight reduction in signal intensity was observed, changing solvent composition from 100% methanol to 100% acetonitrile on observing the molecular ion of cluster $HRu_3(C{\equiv}C\text{-}tert.\text{-}Bu)(CO)_9$. On the other hand, in the case of homometallic

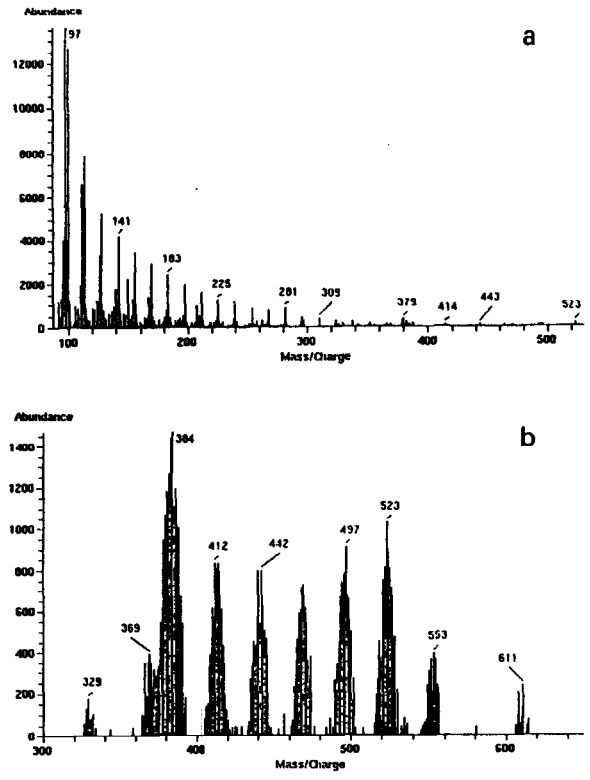

Fig. 4. LC–EI-MS mass spectra of $HRu_3(C{\equiv}C\text{-}tert.\text{-}Bu)(CO)_9$ at different ionization energy: (a) 70 eV; (b) 30 eV. Scan range, 150–750 μ; electron multiplier, 2300 V; positive-ion signal.

triruthenium clusters, it was necessary to use a high percentage of acetonitrile for an optimum elution of compounds.

In order to check the maintenance of the chromatographic resolution when the LC–PB-MS system was used, a UV detector was utilized together with MS for the substitution products of cluster I with the PPh_3 ligands. Fig. 2 provides a comparison of chromatograms of clusters I–IV obtained with UV detection at 265 nm and with the total ion signals from LC–MS, which shows excellent chromatographic fidelity and just a slight loss of resolution in the total-ion chromatogram (TIC) compared with the UV chromatogram. The effects of the nature and the number of the ligands on the separation obtained from LC–UV has already been discussed [16].

The total ion chromatogram of Fig. 2 was obtained by using chemical ionization source monitoring negative-ion signals (NICI mode) of the mixture under conditions reported in the figure. Mass spectra were recorded also in positive-ion (PI) CI mode with the same conditions of reagent gas, source temperature and scan range utilized under NICI conditions. The fragmentation patterns of the compounds in the eluates obtained in the positive-ion mode differ relevantly from that achieved in NICI mode.

Fig. 3 shows a portion of the mass spectra of the parent cluster $HRu_3(C{\equiv}C\text{-}tert.\text{-}Bu)(CO)_9$ in both PICI and NICI modes: the positive-ion spectrum is mainly characterized by the protonated molecular ion ($m/z = 638$), whereas the spectrum obtained by monitoring the negative-ion signal shows more intense fragments corresponding to the loss of up to three CO groups.

The mass spectrum of I was also obtained using electron impact source in two different conditions of ionization energy, as shown in Fig. 4. Using the usual value of collision energy of 70 eV, the compound underwent greater fragmentation than that achieved under milder conditions (30 eV). In this second case, fragments containing the triangular framework of the cluster are present and the gradual loss of all carbonyl groups (up to nine) is favoured. When operating at 30 eV the relative intensities of the ions arising from the breaking of the weaker bonds, namely Ru–CO coordinate bonds, increase and the demolition of the cluster is not observed; therefore lower values of electronic energy are needed to maintain the cluster skeleton.

Concerning the polysubstituted derivatives of cluster I with PPh_3, the PICI mass spectra appeared to be similar for all complexes; in fact they contained only fragments of phosphinic ligands at $m/z = 262$ ($[PPh_3]^+$) and $m/z = 183$ ($[PPh_2 - 2H]^+$), and the ruthenium isotopic pattern was not observed. In the NICI mode the spectra contained several groups of peaks at 28-μ intervals, arising from the loss of CO groups, together with fragments due to the loss of PPh_3 ligands, as shown in Fig. 5: the multiplet of the molecular ion (at m/z 871, 1105, 1338 μ for compounds IIa, III and IV, respectively) is scarcely visible even though always present.

Under reversed-phase conditions, it was observed that the monosubstitution products of the

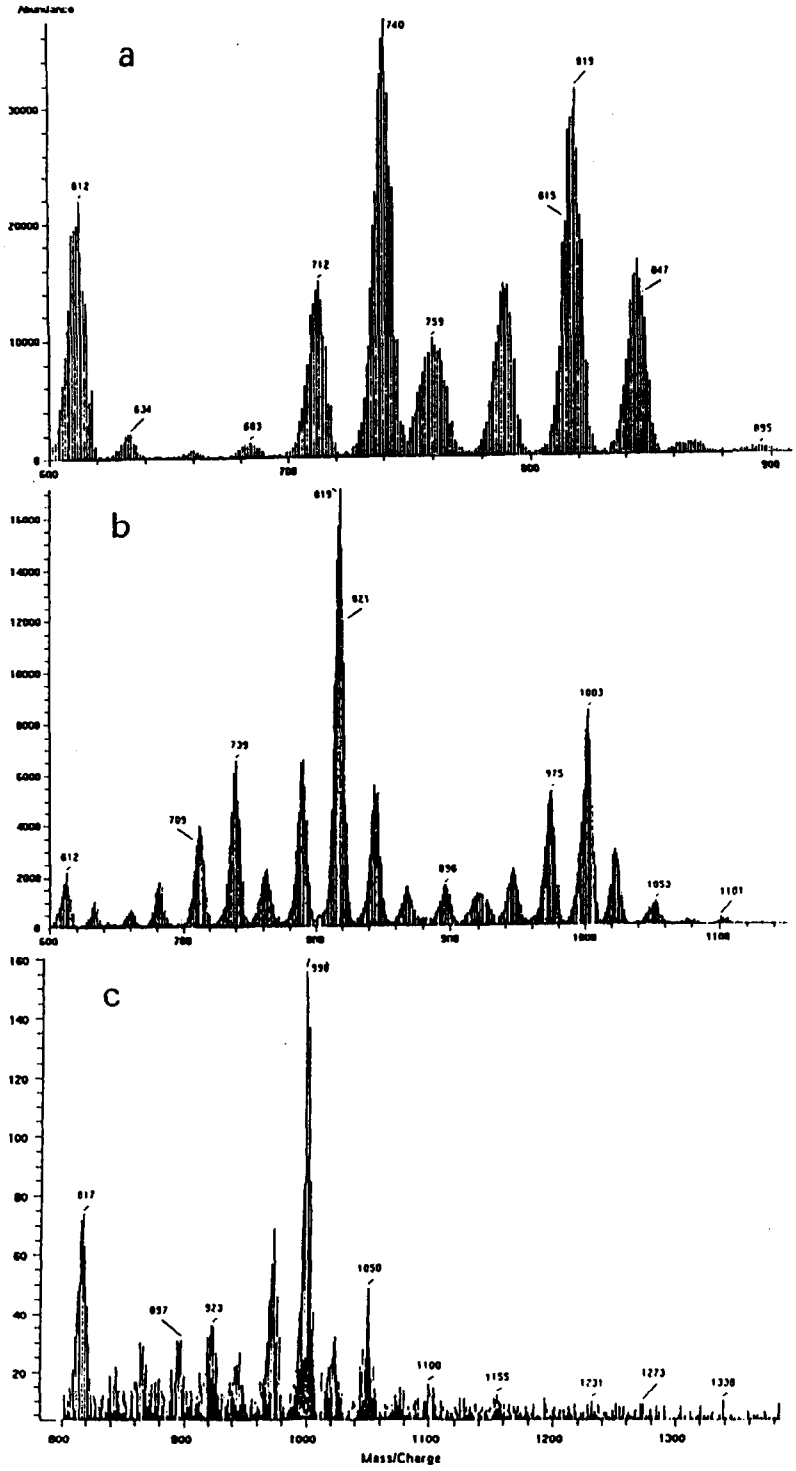

Fig. 5. LC–NICI-PB-MS mass spectra of: (a) $HRu_3(C{\equiv}C\text{-}tert.\text{-}Bu)(CO)_8(PPh_3)$; (b) $HRu_3(C{\equiv}C\text{-}tert.\text{-}Bu)(CO)_7(PPh_3)_2$; (c) $HRu_3(C{\equiv}C\text{-}tert.\text{-}Bu)(CO)_6(PPh_3)_3$. Conditions as in Fig. 2.

TABLE II

MASS SPECTRA OF $HRu_3(C{\equiv}C\text{-}tert.\text{-}Bu)(CO)_8EPh_3$ (E = As, Sb)

m/z	Abundance	Ion
NICI		
583.55	58	$[HRu_3(C{\equiv}C\text{-}tert.\text{-}Bu)(CO)_7]^-$
611.60	100	$[HRu_3(C{\equiv}C\text{-}tert.\text{-}Bu)(CO)_8]^-$
756.05	77	$[HRu_3(C{\equiv}C\text{-}tert.\text{-}Bu)(CO)_5AsPh_2]^-$
784.10	2	$[HRu_3(C{\equiv}C\text{-}tert.\text{-}Bu)(CO)_6AsPh_2]^-$
858.40	4	$[HRu_3(C{\equiv}C\text{-}tert.\text{-}Bu)(CO)_6AsPh_3]^-$
917.40	1	$[HRu_3(C{\equiv}C\text{-}tert.\text{-}Bu)(CO)_8AsPh_3]^-$
554.50	7	$[HRu_3(C{\equiv}C\text{-}tert.\text{-}Bu)(CO)_6]^-$
583.55	56	$[HRu_3(C{\equiv}C\text{-}tert.\text{-}Bu)(CO)_7]^-$
611.60	100	$[HRu_3(C{\equiv}C\text{-}tert.\text{-}Bu)(CO)_8]^-$
802.05	41	$[HRu_3(C{\equiv}C\text{-}tert.\text{-}Bu)(CO)_5SbPh_2]^-$
830.10	4	$[HRu_3(C{\equiv}C\text{-}tert.\text{-}Bu)(CO)_6SbPh_2]^-$
937.50	1	$[HRu_3(C{\equiv}C\text{-}tert.\text{-}Bu)(CO)_7SbPh_3]^-$
963.60	1	$[HRu_3(C{\equiv}C\text{-}tert.\text{-}Bu)(CO)_8SbPh_3]^-$
PICI		
861.05	8	$[HRu_3(C{\equiv}C\text{-}tert.\text{-}Bu)(CO)_6AsPh_3]^+$
888.95	47	$[HRu_3(C{\equiv}C\text{-}tert.\text{-}Bu)(CO)_7AsPh_3]^+$
917.90	100	$[HRu_3(C{\equiv}C\text{-}tert.\text{-}Bu)(CO)_8AsPh_3]^+$
904.75	10	$[HRu_3(C{\equiv}C\text{-}tert.\text{-}Bu)(CO)_6SbPh_3]^+$
933.90	32	$[HRu_3(C{\equiv}C\text{-}tert.\text{-}Bu)(CO)_7SbPh_3]^+$
964.95	100	$[HRu_3(C{\equiv}C\text{-}tert.\text{-}Bu)(CO)_8SbPh_3]^+$

parent cluster I with 15-group donor ligand EPh_3 (E = P, As, Sb) have almost the same retention volumes [16], so that the mass spectra of the compounds were obtained by FIA. In PICI mode, the fragmentation pattern of the derivatives with $AsPh_3$ and $SbPh_3$ ligands (IIb and IIc) showed interesting features compared with the cluster substituted with PPh_3 discussed above: in the first case, the most abundant ions observed were the protonated molecular ions ($m/z = 918$ and $m/z = 965$ μ for IIb and IIc, respectively); the low abundance of the peaks $[M - nCO]^+$ ($n = 1, 2, 3$) indicated a minor stability of the relative fragments. In the mass spectra recorded in NICI conditions, differences in the relative intensities of the peaks were observed: in compounds IIb and IIc, the release of the $AsPh_3$ and $SbPh_3$ ligands is easily obtained, whereas compound IIa showed easier loss of two carbonyls and one phenyl compared with the release of the whole PPh_3 group, suggesting the formation of a diphenylphosphido group bridged to an edge of the cluster [20]; the corresponding ion relative abundances are quoted in Table II.

As for the chromatographic behaviour of the clusters $HRu_3(C{\equiv}CR)(CO)_9$ [R = iso-Pr, *tert.*-Bu, $C(Me)_2OH$, C(Me)(Ph)OH], the reversed-

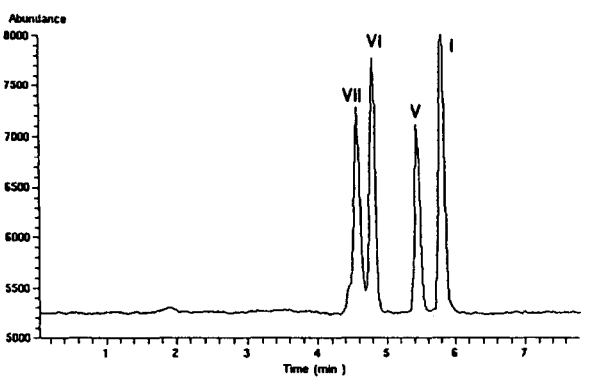

Fig. 6. Total-ion chromatogram of the cluster mixture $HRu_3(C{\equiv}CR)(CO)_9$. Chromatographic conditions: column, LiChrosorb RP-18; mobile phase, acetonitrile–methanol (80:20); flow-rate: 0.8 cm^3/min. MS conditions: source as in Fig. 2; NICI signal; scan range, 150–750 μ.

phase chromatographic separation of the ruthenium derivatives was performed by using an acetonitrile–methanol mixture as eluent: in these conditions, the nature and the electron-donor properties of the R acetylenic substituents appear to be effective in determining the retention order of these structurally related species.

Fig. 6 shows the total ion current profile obtained from the LC–PB-MS system and the mixture of clusters I, V, VI, VII. The CI mass spectrum of the cluster $HRu_3(C{\equiv}C\text{-}tert.\text{-}Bu)(CO)_9$ has been discussed above.

Of particular interest are the chemical ionization mass spectra of clusters V, VI and VII obtained by monitoring both positive- and negative-ion signals.

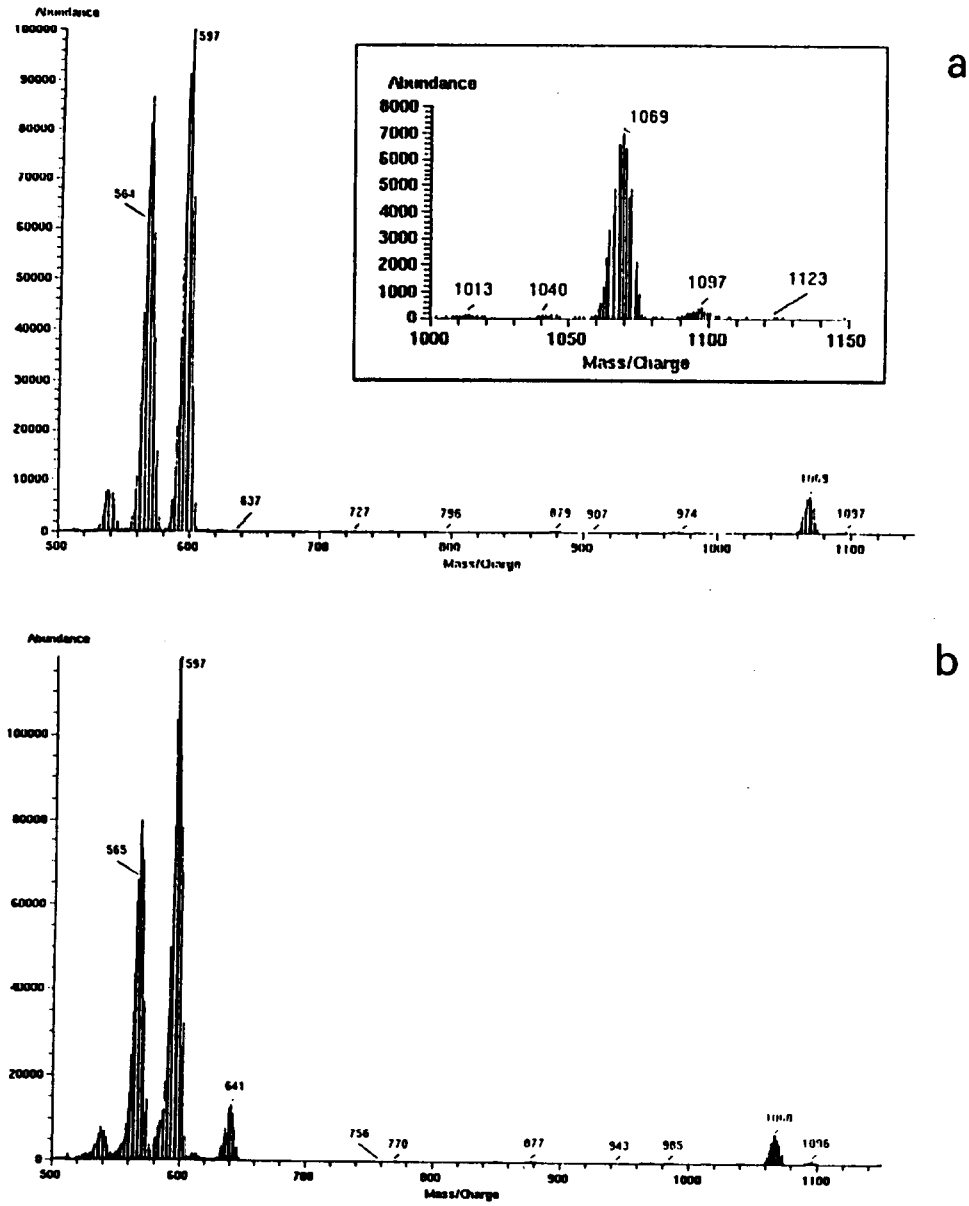

Fig. 7. Negative-ion LC–PB-MS mass spectra of: (a) $HRu_3(C{\equiv}C\text{–}C(Me)_2H)(CO)_9$; (b) $HRu_3(C{\equiv}C\text{–}C(Me)_2OH)(CO)_9$. Same conditions as in Fig. 6.

The fragmentation of V and VI is noteworthy on the NICI mode (Fig. 7); as in the case of the derivative I, the loss of carbonyls (up to three) was favoured and, in the particular case of V, the ion $[M - CO]^-$ ($m/z = 597$) was the most stable, whereas the molecular ion $[M]^-$ represented the most abundant ion for VI. Surprisingly, the mass spectra of both compounds show an isotopic pattern at $m/z = 1069$, suggesting that a dimerization process occurred. A possible explanation is that the acetylide ligand of both clusters generates a dimethyl allenyl fragment by loss of a proton or a hydroxyl group. The allenyl groups of two cluster units can interact in the gas phase, giving rise to dimers with a subsequent release of six CO groups. In contrast, in the signal obtained

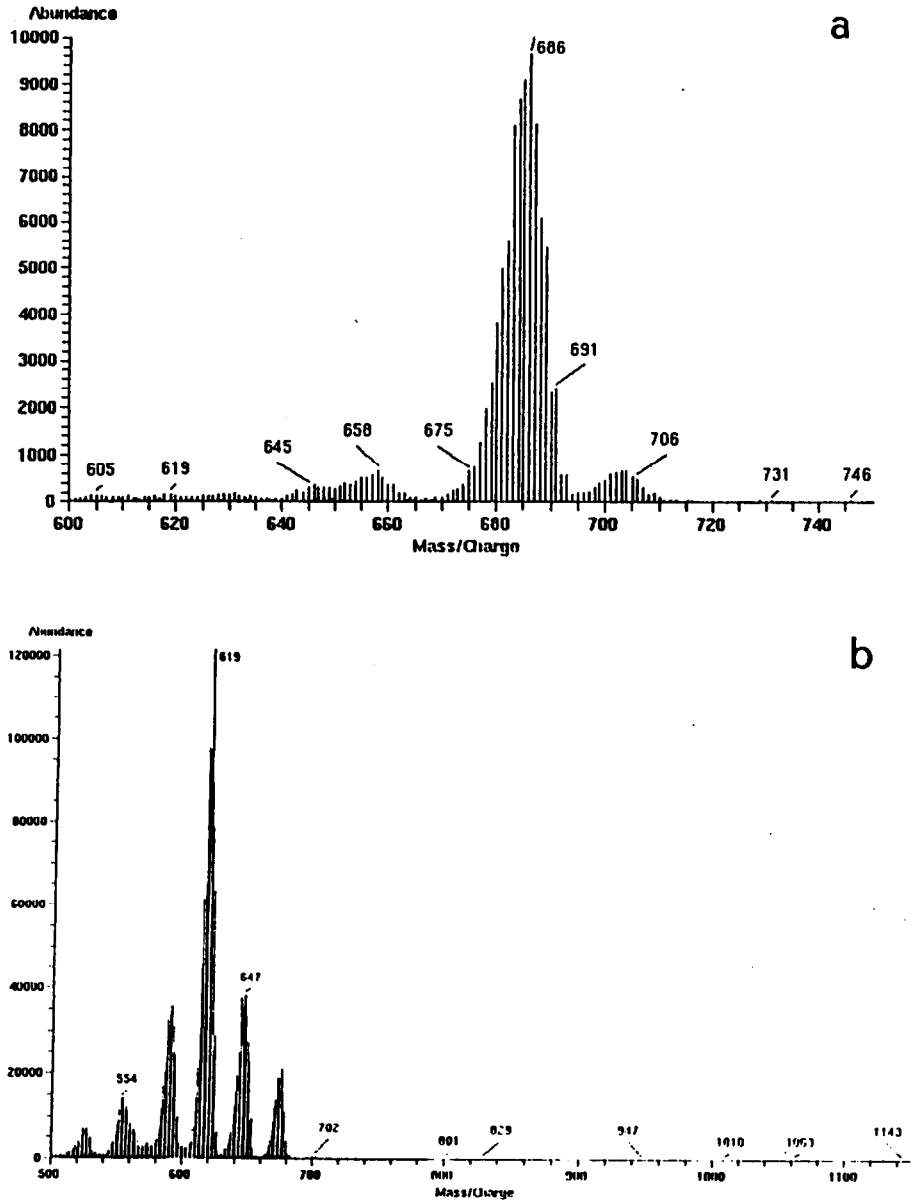

Fig. 8. LC–CI-MS spectrum of $HRu_3(C{\equiv}C{-}C(Me)(Ph)OH)(CO)_9$: (a) positive ion signal; (b) negative ion signal. Same conditions as in Fig. 6.

by monitoring positive ions of the clusters V and VI, fragments at $m/z = 1069$ arising from the dimerization process were not detectable. The PICI mass spectrum of V showed an intense multiplet of molecular ion ($m/z = 626$) and the release of not more than one CO; for compound VI the most abundant fragment was attributable to the ion $[M - OH + C_2H_5]^+ (m/z = 651)$; in addition, adduct ions $[M + C_2H_5]^+$ and $[M + C_3H_5]^+$ were present.

Finally, in the cluster with R = C(Me)(Ph)OH, the easy loss of all nine CO groups was observed under NICI conditions, the ion $[M - 3CO]^-$ being the main fragment (Fig. 8): the different behaviour in release of the carbonyls with respect to the other hydrido–alkyne carbonyl clusters is in agreement with that previously observed [21], namely the loss of the terminal CO groups was found to be effected by the electron-withdrawing power of the substituents on the acetylide.

The figure also contains the positive-ion mass spectrum of compound VII, which shows fragmentation processes different from those of the similar cluster VI having $R = C(Me)_2OH$. In contrast to cluster VI, for which a reaction with the reactant gas together with the loss of an OH group was observed, for compound VII the ion $[M - OH]^+$ ($m/z = 686$) showed the highest stability: this behaviour can be explained on the basis of the presence of the aromatic ring on the acetylide, which stabilizes the system. However, in the case of cluster VII, the release of an OH group does not involve a dimerization process as

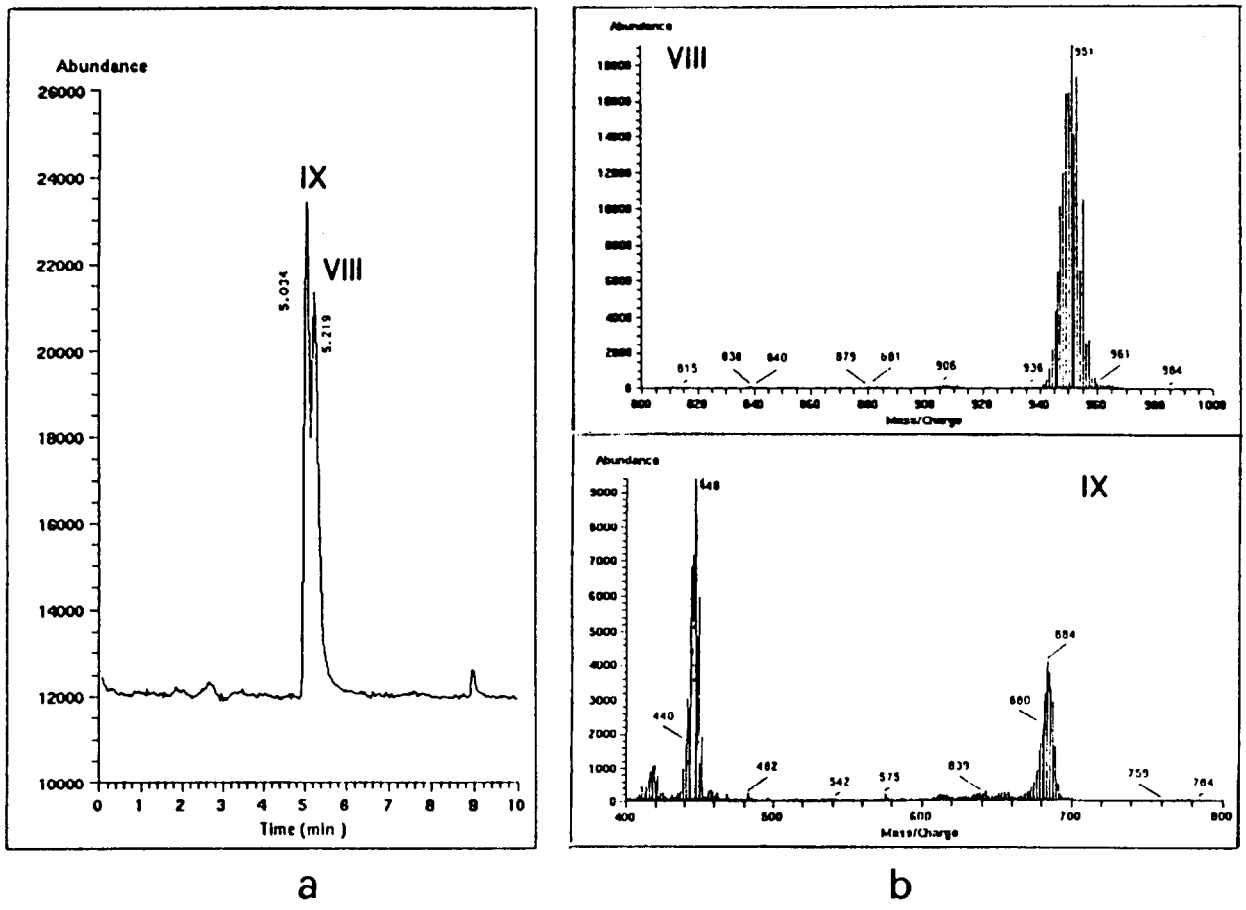

Fig. 9. (a) Separation of the nickel–ruthenium and nickel–osmium heterometallic clusters by LC–PB-MS (TIC) Chromatographic conditions: column, LiChrosorb RP-18; mobile phase, methanol; flow-rate, 0.8 cm^3/min. MS conditions as in Fig. 2, with scan range 100–980 μ. (b) MS spectra (PICI) for the clusters VIII and XI corresponding to the separation in (a).

in the case of the structurally related cluster VI: the allenyl ligand is probably sterically or electronically stabilized by the presence of the aromatic ring. Moreover, adducts with $[C_2H_5]^+$ or $[C_3H_5]^+$, while observed in the case of VI, were not detected for VII.

The chromatographic and mass spectral behaviour of the heteronuclear clusters VIII and IX were investigated. Under reversed-phase conditions, as reported in Fig. 9a, the elution order corresponded to the electronegativity of the metallic centres. Particularly noteworthy are the spectra of the eluates obtained in positive-ion mode (Fig. 9b): in fact, for the nickel–osmium derivative (VIII), only the protonated molecular ion was observed ($m/z = 951$), whereas, surprisingly, the spectrum of the nickel–ruthenium compound (IX) showed, in addition to the molecular ion, an intense signal due to $[NiRu_3(CO)_3]^+$, deriving from the loss of the cyclopentadienyl group and six carbonyls. Also when monitoring the negative-ion signals, the mass spectra of the two clusters presented a different pattern: the nickel–osmium derivative gave rise to the molecular ion ($m/z = 951$) and to the fragment $[M - CO]^-$ with almost the same intensity. The EI mass spectrum obtained by means of direct insertion probe of compound VIII has been reported [15]; in that case the parent ion was not observed and the highest fragment was at $m/z = 920$.

The fragmentation pattern of the nickel–ruthenium cluster was more complex: the loss of up to three CO groups was favoured and the peak corresponding to the molecular-ion ($m/z = 681$) had an intensity of about 50% compared with the most abundant one ($m/z = 653$).

From the results it can be inferred that the LC–PB-MS system can be successfully used even for compounds of particularly complex structure, such as the examined organometallic clusters; for the carbonyl derivatives the NICI mode proves to give more intense spectra and fragmentation patterns more suitable for the identifications.

ACKNOWLEDGEMENT

This work was financially supported by CNR, Italy.

REFERENCES

1 H. Veening, B.R. Willeford, *Adv. Chromatogr.*, 22 (1983) 117.
2 A. Casoli, A. Mangia, G. Predieri and E. Sappa, *J. Chromatogr.*, 355 (1986) 285.
3 A. Casoli, A. Mangia, G. Predieri and E. Sappa, *J. Chromatogr.*, 447 (1988) 187.
4 A. Casoli, A. Mangia, G. Predieri and E. Sappa, *J. Chromatogr.*, 483 (1989) 443.
5 H.G. Ang, W.L. Kwik and W.K. Leong, *J. Organomet. Chem.*, 379 (1989) 325.
6 K.B. Tomer, C.E. Parker, *J. Chromatogr. Biomed. Appl.*, 84 (1989) 189.
7 J.J. Conboy, J.D. Henion, M.W. Martin and J.A. Zweigenbaum, *Anal. Chem.*, 62 (1990) 800.
8 E.C. Huang, T. Wachs, J.J. Conboy and J.D. Henion, *Anal. Chem.*, 62 (1990) 713A.
9 T.D. Behymer, T.A. Bellar and W.L.Budde, *Anal. Chem.*, 62 (1990) 1686.
10 G.J. Van Berkel, S.A. McLuckey and G.L. Glish, *Anal. Chem.*, 63 (1991) 1098.
11 M. Sakairi, A.L. Yergey, K.W.M. Siu, J.C.Y. Le Blanc, R. Guevremont and S.S. Berman, *Anal. Chem.*, 63 (1991) 1488.
12 V. Raverdino and E. Sappa, *Ann. Chim. (Rome)*, 67 (1977) 423.
13 E. Sappa, M.L. Nanni-Marchino and V. Raverdino, *Ann. Chim. (Rome)*, 68 (1978) 349.
14 E. Sappa and V. Raverdino, *Ann. Chim. (Rome)*, 69 (1979) 349.
15 M. Castiglioni, E. Sappa, M. Valle, M. Lanfranchi and A. Tiripicchio, *J. Organomet. Chem.*, 241 (1983) 99.
16 M. Careri, G. Mori, G. Predieri, N. Souza de Rezende and E. Sappa, *J. Chromatogr.*, 634 (1993) 143.
17 C. Jangala, E. Rosenberg, D. Skinner, S. Aime, L. Milone and E. Sappa, *Inorg. Chem.*, 19 (1980) 1571.
18 E. Sappa, A.M. Manotti Lanfredi and A. Tiripicchio, *J. Organomet. Chem.*, 221 (1981) 93.
19 W.V. Ligon, Jr. and S.B. Dorn, *Anal. Chem.*, 62 (1990) 2573.
20 S. Nucciarone, S.A. MacLaughlin, N.J. Taylor and A.J. Carty, *Organometallics*, 7 (1988) 106.
21 O. Gambino, G. A. Vaglio, R. P. Ferrari and M. Valle, *J. Organomet. Chem.*, 76 (1974) 89.